Available online at www.sciencedirect.com
SCIENCE DIRECT®
Journal of Nuclear Materials 329–333 (2004) 1180–1184
journal of nuclear materials
www.elsevier.com/locate/jnucmat

Multiscale modeling of the brittle to ductile transition

S.J. Noronha, J. Huang, N.M. Ghoniem *

Department of Mechanical and Aerospace Engineering, University of California, 420 Westwood Plaza, Los Angeles, CA 90095-1597, USA

Abstract

A recently introduced method of crack representation as a distribution of three-dimensional Volterra dislocations is used in conjunction with two-dimensional dislocation dynamics simulations to study the brittle to ductile transition behavior of Ferritic Steels. The crack-tip plasticity zone is represented as an array of discrete dislocations emitted from crack-tip sources. The dislocations shield the crack and result in an increase of the applied stress intensity for fracture from the pure Griffith value. The crack system responsible for fracture in Ferritic Steels is modeled by a macrocrack and a microcrack in its field. Crack-tip plasticity of microcrack is also modeled by arrays of emitted dislocations. The simulations are performed for different friction stresses corresponding to different yield stresses or temperatures. The brittle to ductile transition fracture toughness curve is obtained and compared to experiments.

1. Introduction

Since the introduction of crack-tip plasticity based models for brittle–ductile transition (BDT) by Rice and Thomson [1], there was an upsurge in the literature on the study of crack-tip plasticity and cleavage crack propagation. In their model they equated the competing forces acting on a dislocation near the crack-tip, and derived a relation for the material to be intrinsically brittle or ductile based the dislocation core width and material parameters. Rice [2] further refined these conditions by obtaining the critical loadings for emission and cleavage. He equated the crack-tip driving forces on distributed shear dislocation cores and cleavage opening, respectively, to the local resistance to dislocation propagation and cleavage along the slip/crack plane. The process (either emission or further opening), which has equal driving force and resistance at the lowest applied load, determines the failure mode. Failure is thus controlled by two material parameters, the surface energy (γ) and the unstable stacking fault energy (γ_{us}) [2]. With increasing computational power, numerical models have been recently introduced at the discrete dislocation dynamics and molecular dynamics levels. Notable among the dislocation dynamics based efforts is the model introduced by Hirsch and Roberts [3,4] to study the effect of dislocation mobility and dislocation source configurations on the BDT of Si and other materials. This method has recently been used to model the initiation of cleavage of Ferritic steels at low temperature [5]. A finite slit crack loaded under triaxial stress is used to study the cleavage initiated by brittle precipitates. The model predicts the constancy of microscopic cleavage fracture stress observed in experiments, resulting in reasonable quantitative agreement with experiments [6]. Several groups conducted large-scale atomistic simulations of crack-tip plasticity [7,8]. Shastry and Farkas [9] developed an embedded atom method based potential for α-Fe and studied the dislocation emission from of a slit crack. Recently, the effect of dislocation blocking on crack-tip behavior of α-Fe was studied using both atomistic and dislocation dynamics simulations [10].

Clearly crack-tip plasticity is a multiscale phenomenon. The macroscopic continuum mechanics dictates the stress state around the crack. The plastic zone around

* Corresponding author. Tel.: +1-310 825 4866; fax: +1-310 206 4830.
E-mail address: ghoniem@ucla.edu (N.M. Ghoniem).

0022-3115/$ - see front matter © 2004 Elsevier B.V. All rights reserved.
doi:10.1016/j.jnucmat.2004.04.266

the crack-tip is controlled by the long-range elastic interactions like, crack–dislocation, dislocation–dislocation/particle/grain boundaries (mesoscopic) and short-range nonlinear interactions like dislocation reactions (atomistic). The mobility of the dislocation on the other hand is controlled by the dislocation core behavior, which needs detailed modeling of bonds at the electronic level. Hence a complete description of fracture requires knowledge of length scales ranging from macroscale to electronic.

In spite of the progress in understanding the fundamentals of fracture, the BDT of practical materials still relies heavily on the continuum methods. To explain the extremely high cleavage fracture toughness measured in Ferritic Steels at low temperatures, Orowan [11] postulated that the fracture in ferritic steels could occur due to cleavage originated from microcracks ahead of the macrocrack. This was later confirmed by experiments [12,13] and it is now a well accepted fact that fracture in steels is initiated by cracks in precipitates and propagation of these microcracks into the matrix is the controlling step in the fracture. Ritchie, Knott and Rice (RKR) [14] used finite element method (FEM) and asymptotic solutions of crack-tip with small geometric change to simulate the plastic zone, a critical tensile stress on a brittle particle situated at a *distance* ahead of the macrocrack is used as the failure criterion. This distance is essentially a fitting parameter and RKR [14] used a value equal to/or twice the average grain diameter. The model successfully predicts lower-shelf fracture toughness, but fails to predict the upturn near the transition temperature. Statistical models were introduced to predict brittle–ductile transition of steels starting with Curry and Knott [13], most notable among them were by Beremin [15] and Wallin et al. [16]. In both these models FEM solution of crack-tip plasticity was used. In Beremin model [15], the maximum principal stress is calculated for each volume element in the plastic zone and a probability of failure is assigned. The total probability of failure is then obtained by summing over the entire plastic zone. Wallin et al. [16] extended the modeling with some success to the transition region by considering variation of *effective surface energy* ($\gamma_s + \gamma_p$) (where γ_s is the true surface energy and γ_p the plastic work done during propagation) with temperature. This model eventually led to the master Curve (MC) hypothesis, which predicts that brittle–ductile transition of all ferritic steels follows a universal curve [16,17]. Odette and He [18] used a microscopic fracture stress varying with temperature to explain the master curve. Even though MC is used to check the reliability of structures under irradiation [19], a clear understanding of the physical basis of this methodology is still lacking [20]. Here, we present preliminary results on the modeling of lower shelf and the master curve based on discrete dislocation simulation.

In the next section, we outline the details of the model and the calculation procedure used. Section 3 describes the results obtained by our methodology. We also compare our predictions with experimental results reported in the literature. Finally in Section 4 we summarize our results and discuss possible improvements to our model.

2. Model and method of calculation

2.1. Dislocation based crack-tip: 3D simulation

A distribution of *Voltera crack dislocations* represented by parametric curves [22] is used to simulate 3D cracks. In this methodology [21], the image force effects on crystal dislocations due to the crack surfaces will be accounted for by the interaction between *Voltera crack dislocations* and crystal dislocations. Fig. 1(a) shows the reconstructed crack opening displacement obtained for a 'slit crack' simulated, note the depth of crack is 10 times its width, hence can be compared with 2D slit crack. In the simulation, small dislocation segments of 200a, where a is the lattice constant, were placed near the crack-tip and their evolution under the crack-tip loading is studied. Note that dislocation nucleation is a two stage processes: (a) formation of embryo half loops at sources like ledges or other imperfections at the crack front (b) growth of these half loops to form dislocations that cover the crack front. We deal with only the second stage in our simulation.

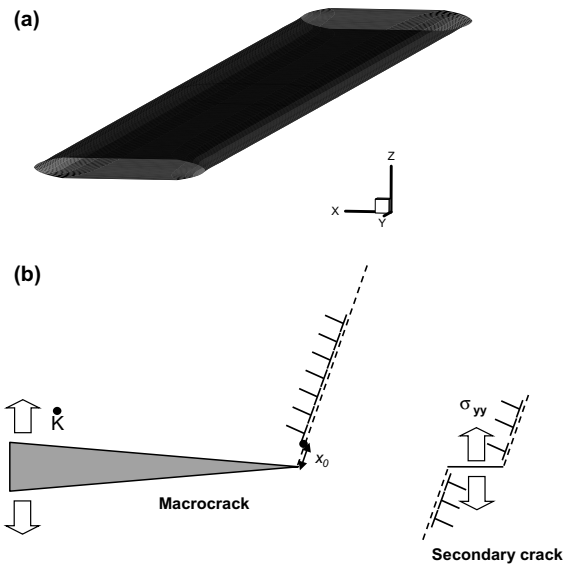

Fig. 1. (a) The reconstructed crack shape obtained from the distribution of 3D Voltera crack dislocations and (b) the geometry of crack and dislocations used in the 2D coupled macrocrack–microcrack simulation model.

2.2. Coupled macrocrack–microcrack: 2D simulation

The geometry of the 2D model used is shown in Fig. 1(b). A semi-infinte crack (macrocrack) with a finite crack (microcrack) situated ahead of it in its crack plane is loaded. Note that in this configuration, the load at the microcrack will be the sum of the elastic stress field from the macrocrack and that due the dislocations in the plastic zone. This field can be approximated to that of a hardening material with small scale yielding at the crack-tip [4]. A dislocation source is assumed to exist at a distance x_0 from, and situated on a slip plane oriented at an angle and passing through, each crack-tip. A dislocation is emitted when the resolved shear stress on a dislocation at x_0 is greater than τ_f. Where τ_f is the friction stress used and is chosen to be equal to $\sigma_y/\sqrt{3}$, where σ_y corresponds to the uniaxial yield stress at a given temperature. The temperature dependence of fracture toughness is then obtained by inputting the corresponding friction stress value. The resolved shear stresses are obtained using expressions based on derivations for semi-infinite crack [23] and finite crack [24]. The emitted dislocations move along the slip plane away from the crack-tip, and the stress at the source increases until another dislocation is emitted. (For each positive dislocation emitted, a negative one is assumed to move into the crack.) In the case of microcrack, the sources on opposite sides of the crack are at equivalent positions x_0 and operate simultaneously. (This ensures that no net Burgers vector remains in the crack). The dislocations are assumed to move with a velocity v given by

$$v_{x_i} = \left(\frac{|\tau_{x_i}|}{\tau_0}\right)^m v_0 \left(\frac{|\tau_{x_i}| - \tau_f}{\tau_{x_i}}\right) \quad (1)$$

for $|\tau_{x_i}| > \tau_y$ and $v = 0$ for $|\tau_{x_i}| < \tau_f$. The computations were carried out with $m = 2.67$ and $v_0 = 4.5 \times 10^{-10}$ ms^{-1}, appropriate to the velocities of screw dislocations in iron at 273 K [25]. During the simulation, the applied stress intensity is increased in small increments and the positions of dislocations are determined. It is found that the dislocations reach near equilibrium positions. It should be noted that with the dislocations in near-equilibrium positions, the temperature and strain–rate dependence of K_F, the numbers of dislocations emitted at fracture, and the plastic zone size are determined only by the temperature and strain-rate dependence of the yield stress, σ_y. The emitted dislocations shield the crack from external load, by compressive stresses they exert at the crack-tip. The shielding stress intensity factor for each dislocation (K_D) is calculated at each crack-tip. The expressions for semi-infinite were used from [23] and that for finite crack from [24] and the total net shielding stress intensity factor for each crack-tip is obtained by summing the K_D from respective dislocation arrays. The fracture criterion for this model is a critical crack-tip stress intensity of the microcrack. Thus, when $k = K_{IC}$, cleavage fracture of the matrix is assumed to occur; the applied load at the macrocrack, then gives the critical loading for fracture propagation K_F and the microscopic cleavage fracture stress (σ_F) is the net tensile stress due to the macrocrack field and the array of dislocations emitted from it.

3. Results and discussion

3.1. Crack-tip simulation using 3D dislocations

As shown in Fig. 2(a), dislocations were nucleated at isolated sites with separating distance $500a$; all of them are initially straight dislocation segments gliding on (1 0 1)-plane, with length $200a$. The crack system is chosen as (1 0 0)[0 1 0]. Once nucleated, these dislocations will bow out with two ends sliding along the crack-tip, until it merges with neighbors. As shown in Fig. 2(b), at $t = 20.518$ s, one long straight dislocation is formed, and will glide away from the crack with its two ends sliding along the two side. Here we assume that the nucleation energy is zero, or it means at the nucleation site, there is always a dislocation nucleus, and once there is enough stress to drive them away, the nuclei become a crystal dislocation. It can be seen that beyond a certain distance, here $80a$; the dislocation remains parallel to the crack front and can be approximated by 2D dislocations. This distance of $80a$ is used in the following 2D simulations as the 'source distance' from the crack-tip.

3.2. Coupled macro–micocrack simulations using 2D dislocations

A microcack of size 1 μm is placed at a distance of 10 μm from the macrocrack-tip (10 μm is the average distance obtained in [13], with which we compare our results). The value of x_0 used in simulation is $80a$, where a is the lattice constant; the slip planes are oriented at an angle of 70.5° to the crack plane. Fig. 3(a) shows a typical behavior of the crack-tip stress intensity at the

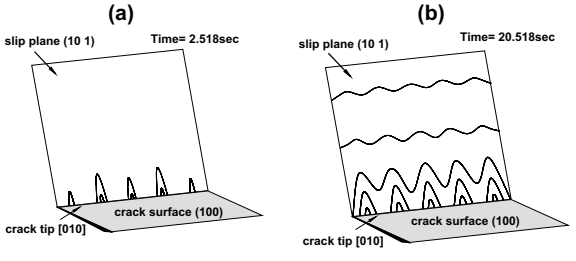

Fig. 2. Evolution of dislocation configurations in Iron single crystals at 500 K; as time progresses (from (a) and (b)) the dislocation loops turn parallel to the crack front.

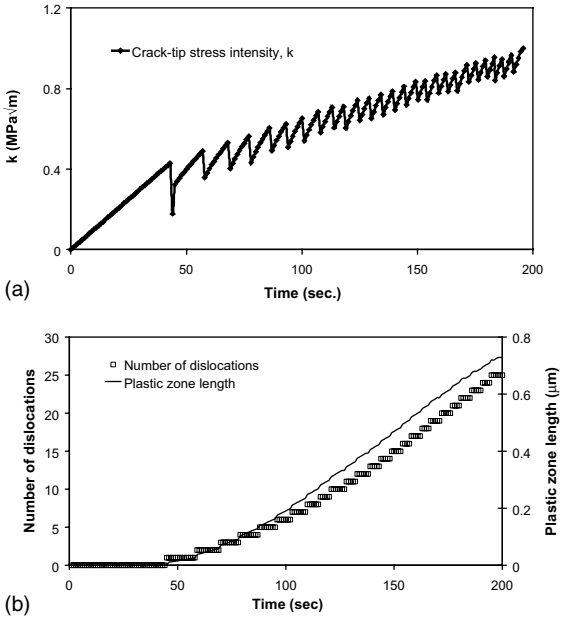

Fig. 3. (a) The stress intensity at the micocrack-tip and as a function of simulation time; crack size = 1 μm, yield stress = 800 MPa; and (b) the number of dislocations and the plastic zone length at the microcrack-tip as a function of simulation time; crack size = 1 μm, yield stress = 800 MPa.

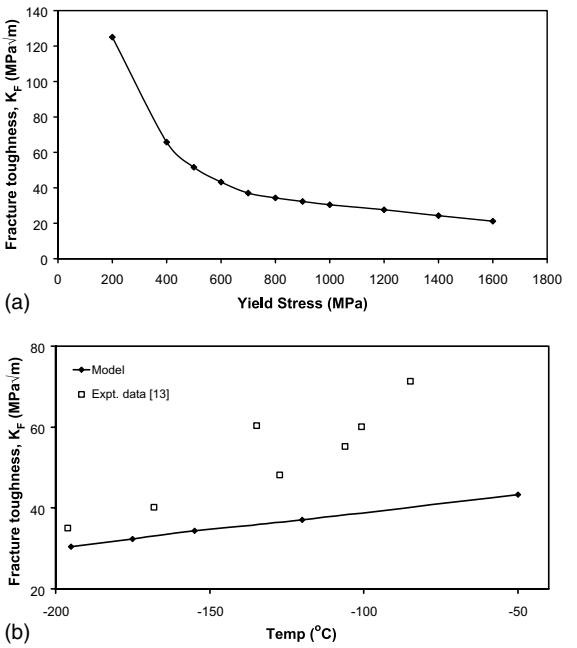

Fig. 4. (a) The fracture toughness as a function of yield stress, the criterion of fracture is the critical crack-tip stress intensity of the microcrack ($k = 1$ MPa $\sqrt{}$m) and (b) the fracture toughness values from above Fig. 4(a) mapped to temperature for the limited range of yield stress–temperature relation and the experimental fracture toughness.

microcrack (k) while it is loaded. The fracture criterion in this case is k reaching a critical value (here equal to 1 MPa $\sqrt{}$m, which is the K_{IC} value if we assume pure cleavage of Fe). Each drop in the curve corresponds to new dislocation generation at the microcrack-tips, and we can see that the emitted dislocations shield the microcrack and enhance the stress required for cleavage. The total amount of shielding due to all dislocations can be interpreted as the *plastic work during crack propagation*. In this case, the microcrack size is 1 μm, the yield stress is 800 MPa and the rate of loading, $dK/dt = 0.01$ MPa $\sqrt{}$m s^{-1}. Fig. 3(b) shows the number of dislocations and length of the plastic zone developed at the microcrack-tip with the progress in simulation.

The variation of microscopic cleavage fracture stress (σ_F) (that is the net tensile stress at the microcrack due to the stress field of macrocrack and the dislocation array developed at the macrocrack, at fracture) as a function of yield stress is less than 10% for the range of yield stress studied (200–1600 MPa), and is consistent with the experimental observations. The variation of macroscopic fracture toughness, K_F as a function of yield stress is shown is Fig. 4(a). There is sharp increase in the fracture toughness at low yield stresses, which correspond to the transition from brittle to ductile behavior. In Fig. 4(b) portion of the fracture toughness curve in Fig. 4(a) is mapped to temperature using experimental yield stress [13] to obtain the brittle–ductile transition curve. We can see that model fits well to experimental results at lower shelf fracture toughness; however, it does not predict the sharp upturn at the transition. Note, the yield stress range to which we could map the data is very narrow (600–1000 MPa), due the unavailability of data for broader temperature range. Also our model does not consider dislocation multiplication, which will have significant effect at lower yield stress or high temperature regime.

4. Summary and conclusions

The evolution of dislocation loops originating near crack-tips is studied using 3D dislocation dynamics. In the simple configuration, chosen it is found that the loop becomes parallel to the crack front beyond a certain distance. This distance is used as the source distance in the 2D simulations. The 2D dislocation dynamics simulation is used to study the crack system involved in the fracture of ferritic steels; macrocrack with a microcrack ahead of it. In this model the postulated amount of *plastic work done during propagation* is equated to the total shielding at the crack-tip due to dislocations. The crack-tip plastic behavior and the lower shelf values of brittle to ductile transition curve predicted have good

agreement. However, the model does not predict the sharp upturn near the transition temperature. It should be noted that our simulations do not involve dislocation multiplication processes, which become significant at higher temperatures near the transition temperature. This drawback could be overcome by carefully devising local rules using 3D dislocation simulations, which is now in progress.

References

[1] J.R. Rice, R. Thomson, Philos. Mag. 29 (1974) 73.
[2] J.R. Rice, J. Mech. Phys. Solids 40 (1992) 239.
[3] P.B. Hirsch, S.G. Roberts, Philos. Mag. A 64 (1991) 55.
[4] P.B. Hirsch, S.G. Roberts, Philos. Trans. R. Soc. London A 355 (1997) 1991.
[5] S.G. Roberts, S.J. Noronha, A.J. Wilkinson, P.B. Hirsch, Acta Mater. 50 (2002) 1229.
[6] P. Bowen, S.G. Druce, J.F. Knott, Acta Metall. 34 (1986) 1121.
[7] F.F. Abraham, Europhys. Lett. 38 (1997) 103.
[8] S.J. Zhou, D.M. Beazley, P.S. Lomdahl, B.L. Holian, Phys. Rev. Lett. 78 (1997) 479.
[9] V. Shastry, D. Farkas, Model. Simulat. Mater. Sci. Eng. 4 (1996) 473.
[10] S.J. Noronha, D. Farkas, Mater. Sci. Eng. A 365 (2004) 156.
[11] E. Orowan, Trans. Inst. Eng. Shipbuilders Scotland 89 (1945) 165.
[12] C.J. McMahon Jr., M. Cohen, Acta Metall. 13 (1965) 591.
[13] D.A. Curry, J.F. Knott, Met. Sci. 13 (1986) 341.
[14] R.O. Ritchie, J.F. Knott, J.R. Rice, J. Mech. Phys. Solids 21 (1973) 395.
[15] F.M. Beremin, Metall. Trans. A 14 (1983) 2277.
[16] K. Wallin, T. Saario, K. Törrönen, Met. Sci. 18 (1984) 13.
[17] D.E. McCabe, J.G. Merkle, K. Wallin, in: P.C. Paris, K.L. Jerina (Eds.), Fatigue and Fracture Mechanics: 30th Volume, ASTM STP, 1360, ASTM, West Conshohocken, PA, 2000, p. 21.
[18] G.R. Odette, M.Y. He, J. Nucl. Mater. 283–287 (2000) 120.
[19] ASTM Standard Test Method E 1921-02, Annual Book of ASTM Standards, vol. 03.01, 2002.
[20] M.E. Natishan, M.T. Kirk, in: P.C. Paris, K.L. Jerina (Eds.), Fatigue and Fracture Mechanics: 30th Volume, ASTM STP, 1360, ASTM, West Conshohocken, PA, 2000, p. 51.
[21] J. Huang, N.M. Ghoniem, to be published.
[22] N.M. Ghoniem, S.H. Tong, L. Sun, Phys. Rev. B 61 (2000) 913.
[23] V. Lakshmanan, J.C.M. Li, Mater. Sci. Eng. A 104 (1988) 95.
[24] S. Wang, S. Lee, Mater. Sci. Eng. A 130 (1990) 1.
[25] H. Saka, K. Nada, T. Imura, Cryst. Lattice Defects 4 (1973) 45.